Donor-acceptor pairs in the confined structure of ZnO nanocrystals

Serguei B. Orlinskii, Hubert Blok, and Jan Schmidt
Department of Molecular Physics, Huygens Laboratory, Leiden University, Post Office Box 9504, 2300 RA Leiden, The Netherlands

Pavel G. Baranov
A.F. Ioffe Physico-Technical Institute, Russian Academy of Sciences, 194021 St. Petersburg, Russia

Celso de Mello Donegá and Andries Meijerink
Debye Institute, Utrecht University, Utrecht, The Netherlands

(Received 7 February 2006; revised manuscript received 1 June 2006; published 12 July 2006)

The electron paramagnetic resonance signal of an exchange-coupled pair consisting of a shallow interstitial Li donor and a deep Na-related acceptor has been identified in ZnO nanocrystals with radii smaller than 1.5 nm. From electron nuclear double resonance experiments it is concluded that the deep Na-related acceptor is located at the interface of the ZnO core and the $Zn(OH)_2$ capping layer, while the Li donor is in the ZnO core.

DOI: 10.1103/PhysRevB.74.045204 PACS number(s): 71.55.Gs, 61.72.Vv, 76.30.Da, 76.70.Dx

INTRODUCTION

Exchange-coupled donor-acceptor (or electron-hole) pairs in semiconductors are observable in the electron paramagnetic resonance (EPR) spectrum when the electronic wave functions of the donor and acceptor start to overlap significantly. In intentionally doped semiconductors these pairs are difficult to observe because the concentration of donors and acceptors has to be relatively high. An interesting case is formed by the Frenkel pairs as observed for instance in ZnSe.[1] These pairs consist of a Zn vacancy and a Zn interstitial (V_{Zn}-Zn_i) which stabilize at a mutual distance that is so short that the exchange interaction, resulting from the overlap of the wave functions, forms the dominant term in the spin Hamiltonian. This Hamiltonian then takes the form

$$H = g_D \beta_e \boldsymbol{B} \cdot \boldsymbol{S}_D + g_A \beta_e \boldsymbol{B} \cdot \boldsymbol{S}_A + J \boldsymbol{S}_D \cdot \boldsymbol{S}_A .$$

Here the first two terms on the right side describe the Zeeman energies of the donor and acceptor with electron spins $S_D = S_A = \frac{1}{2}$ and g factors g_D and g_A. J is the isotropic exchange interaction between the donor and the acceptor. For large values of J such that

$$|J| \gg |g_D - g_A| \beta_e B,$$

where β_e and B are the Bohr magneton and the magnetic field, respectively, a single EPR signal arises at the mean g value $g_P = (g_D + g_A)/2$.[1,2].

In nominally undoped ZnO crystals the EPR signal of shallow interstitial hydrogen donors has recently been observed.[3] The Bohr radius of the hydrogenlike $1s$ wave function of this interstitial hydrogen donor $a_D = 1.5$ nm. As yet only deep acceptors with a localized wave function have been detected in this material. When the Bohr radius a_D of the donor is much larger than the Bohr radius a_A of the acceptor the exchange interaction between the shallow donor and the deep acceptor depends exponentially on the donor-acceptor distance, i.e., $J = J_0 \exp(-2r/a_D)$,[4] where J_0 is the limiting exchange interaction for $r = 0$. The value of J_0 can be estimated from a comparison with the particular case of the self-trapped exciton in AgCl. This self-trapped exciton consists of a hole with a deep level localized on an Ag^+ site (Ag^{2+} center) and an electron shallowly bound to this center. The Bohr radius of the hydrogenlike $1s$ wave function of this electron, a_D, is also1.5 nm and it was found that $J_0 = 5.37$ cm^{-1}.[5] When using this value of J_0 we derive that the distance between shallow donors and deep acceptors in ZnO should be smaller than 2 nm in order to observe the pair signals. For the typical concentrations of 10^{16}–10^{17} cm^{-3} of these donors and acceptors in bulk ZnO their average distance is so large that the probability to find donor-acceptor pairs with an appreciable exchange interaction is negligible.

The question arises whether donor-acceptor pairs can be observed in nanocrystals of ZnO. Such crystals can routinely be produced with radii smaller than 2 nm and if donors and acceptors could be introduced in these particles the confinement is then expected to lead to the formation of donor-acceptor pairs. Recently we have demonstrated that ZnO nanocrystals can be doped with shallow, interstitial Li or Na donors.[6,7] A prerequisite for the observation of the EPR signal of the unpaired spin of these donors at liquid-helium temperatures is that the nanocrystals are first illuminated with above-band-gap light. This observation shows that there must be deep acceptors present in the nanocrystals that capture the thermally excited donor electrons at room temperature. Apparently these electrons remain frozen at the acceptor when the material is cooled in the dark to low temperature. The above-band-gap light transfers the electron from the acceptor to the donor and makes both sites paramagnetic, but even in ZnO nanocrystals with a radius as small as 1.7 nm it was impossible to observe signals of exchange-coupled donor-acceptor pairs. In this paper we show that for ZnO nanocrystals with radii smaller than 1.5 nm we can observe EPR signals that can be attributed to pairs formed by the shallow Li donor and the deep acceptor.

EXPERIMENTAL

The measurements were carried out on dry powders of free-standing, $Zn(OH)_2$-capped, ZnO nanocrystals doped

with shallow Li donors. Samples of nanocrystals with average radii of 1.7, 1.3, and 1.17 nm (10% dispersion) were prepared following the method reported in our previous study.[6,7] This method is based on the hydrolysis of Zn^{2+} ions in absolute ethanol using $LiOH \cdot H_2O$, followed by precipitation with heptane. After rinsing with heptane and acetone the powders are dried under vacuum and stored in sealed bags at −15 °C. The average nanocrystal sizes were estimated by x-ray powder diffraction (XRD), uv-visible absorption spectroscopy, and transmission electron microscopy (TEM).[6,7] The average thickness of the $Zn(OH)_2$ shell was estimated by comparing the sizes determined by XRD (the size of the crystalline ZnO core) and by TEM (the total nanoparticle size), which yields 0.3±0.15 nm corresponding to 1±0.5 monolayer. The EPR and electron nuclear double resonance (ENDOR) experiments were performed at 1.6 K on a pulsed 94.9 GHz EPR/ENDOR spectrometer[8] and on a similar system operating at 275 GHz.[9,10] The EPR spectra were recorded by monitoring the electron spin echo (ESE) signal following a microwave $\pi/2$- and π-pulse sequence. The ENDOR spectra were obtained by monitoring the intensity of the stimulated echo, following three microwave $\pi/2$ pulses, as a function of a radio-frequency pulse applied between the second and third microwave pulses.[11]

The thermal behavior of the paramagnetic centers was studied by means of a series of isochronal-anneal experiments. The nanocrystals were illuminated with above-band-gap light to create paramagnetic electron and hole centers. This illumination was followed by a series of 30 minutes anneals at successively higher temperatures. After each anneal, the EPR spectrum was recorded at 1.5 K at 94.9 GHz or at 8 K at 275 GHz to ensure a reliable comparison of the EPR spectra.

Photoluminescence (PL) and thermoluminescence (TL) spectra were acquired using a 450 W Xe lamp and a double-grating 0.22 m monochromator for excitation. The emitted light was collimated into an optical fiber cable leading to a 0.3 m monochromator (Acton Pro SP-300i, 150 lines/mm grating, blazed at 500 nm) and detected by a liquid N_2-cooled Princeton Instruments charged-coupled device (CCD) camera (1024×256 pixels). The sample was mounted in a He-flow cryostat allowing for measurements in the 4.2 to 300 K temperature range. The samples were illuminated with 300 nm light for 3 hours at 4.2 K prior to the TL measurements. The heating rate was 2 K/min and the spectra were integrated during 60 s at each temperature.

RESULTS AND DISCUSSION

Figure 1(a) shows an ESE-detected EPR spectrum at 94.9 GHz at 1.6 K and Fig. 1(b) a similarly detected EPR spectrum at 275 GHz at 8 K of a dry powder sample of Li-doped ZnO nanocrystals with a radius of 1.3 nm after continuous ultraviolet (UV) illumination during 30 minutes. The spectrum in Fig. 1(a) looks very similar to the one observed at 95 GHz for ZnO nanoparticles with a radius of 1.7 nm.[6] The signal I belongs to the shallow interstitial Li donor and signal II to a deep Na-related center. The important difference is that a new EPR signal (III) is visible halfway between the signal of the shallow Li donor (I) and the signal of the deep Na-related center (II). Signal III is attributed to an exchange-coupled pair formed by the shallow Li donor and the deep Na-related center.

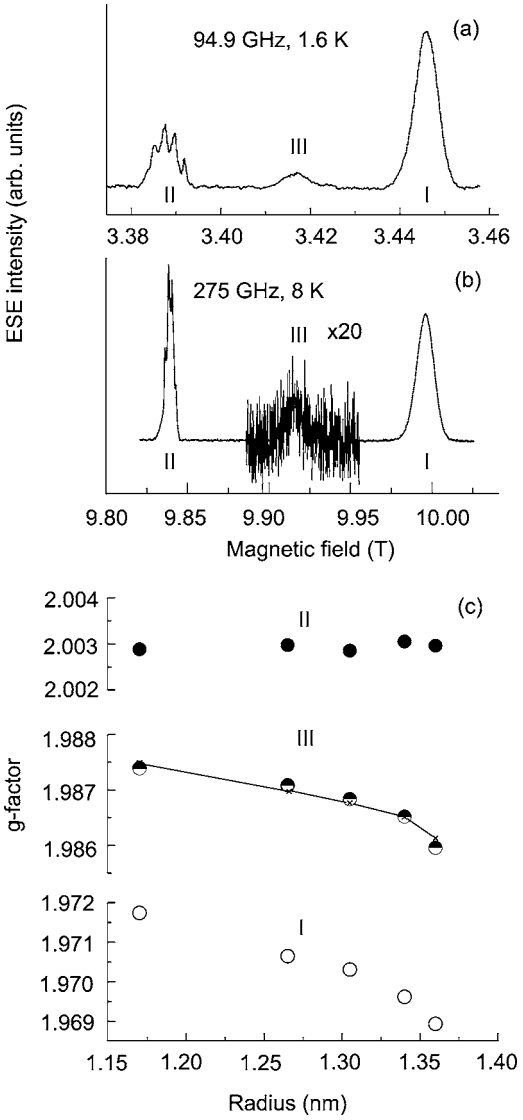

FIG. 1. (a) The ESE-detected EPR spectrum at 94.9 GHz of a dry powder sample of Li-doped ZnO nanocrystals with an average radius of 1.3 nm at 1.6 K after UV illumination during 30 min. The signals marked I and II arise from an isolated shallow Li-donor and a deep Na-related acceptor, respectively. A donor-acceptor pair formed by the shallow Li-donor and the deep Na-related acceptor causes the EPR signal marked by III. (b) The same ESE-detected EPR spectrum as in (a) but recorded at a frequency of 275 GHz at 8 K. It is seen that the separation of the signals I and II of the shallow donor and the deep Na-related acceptor is increased by the ratio of the EPR frequencies but that the pair signal III remains exactly halfway between signal I and II. (c) The variation of the g values of the EPR signals I, II, and II as a function of the radius of the ZnO nanocrystals.

In Fig. 1(c) the variation of the g values of signals I, II, and III is presented as a function of the radius of the ZnO nanoparticles. It is seen that the g value of signal II is independent of the size of the nanoparticles, typical for a deep

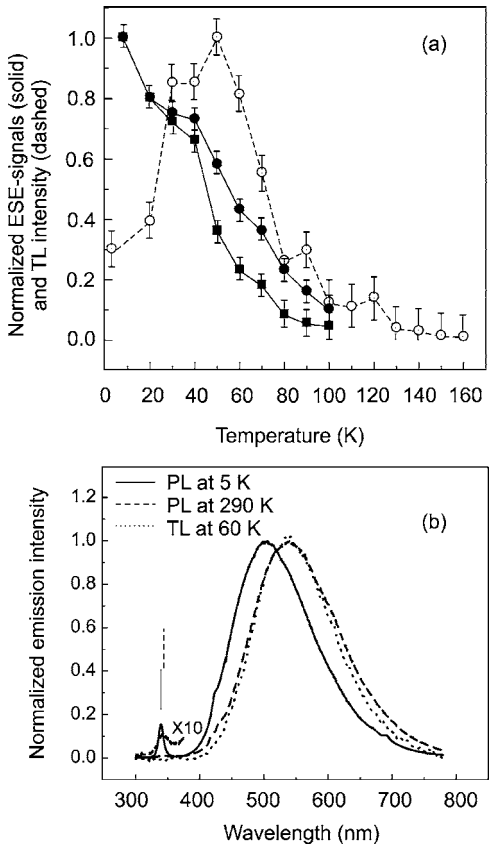

FIG. 2. (a) The EPR intensities at 275 GHz and at 8 K of signal I of the shallow Li donor (filled circles) and signal II of the deep Na-related acceptor (filled squares), normalized to their original 8 K values for Li-doped ZnO nanocrystals with an average radius of 1.3 nm after an anneal at higher temperatures. The dashed line and the open circles indicate the relative intensity of the thermoluminescence at various temperatures after UV illumination at 300 nm during 3 h at 4.2 K. (b) The photoluminescence spectra at 5 K (solid line) and at 290 K (dashed line) and the thermoluminescence spectrum at 60 K (dotted line) for Li-doped ZnO nanocrystals with an average radius of 1.3 nm. The exciton line at 290 K is shown with an amplification by a factor of 10. The exciton lines in the PL spectra are marked by bars: the solid bar indicates 5 K and the dashed bar 290 K.

center with a localized wave function. The variation of the g value of signal I results from the confinement effect on the wave function of the shallow Li donor.[6,7] It is seen that the variation of the g value of signal III is half that of the variation of the g value of signal I. We use this observation as a support for the assignment of signal III to an exchange-coupled pair between the shallow Li donor (I) and the deep Na-related acceptor (II).

Further support for the assignment of signal II as arising from a deeply trapped hole is provided by the isochronal annealing experiments. The thermally induced reduction in concentration of the paramagnetic donors and acceptors was monitored by the change in intensity of the EPR signals. In Fig. 2(a) the results of these measurements at 275 GHz are plotted and it is seen that qualitatively the reduction in intensity of signal I of the shallow Li donors (filled circles) and the signal II of the Na-related centers (filled squares) is similar. As indicated in Fig. 2(a) the intensity of the two signals starts to reduce substantially at 50 K. After the annealing at 150 K the two signals have completely disappeared. The observations lend support to the idea that the thermally released donor electron is captured by the Na-related center making both centers nonparamagnetic. We conclude that the deep Na-related center must have acceptorlike properties.

The recombination of the donors and acceptors as observed in the EPR-detected annealing experiments is accompanied by an intense thermoluminescence (TL). In Fig. 2(b) the thermoluminescence spectrum at 60 K is shown together with the photoluminescence (PL) spectra at 5 K and at 290 K for Li-doped ZnO nanocrystals with an average radius of 1.3 nm. Two emission bands are observed in the photoluminescence spectra: a relatively weak and narrow UV exciton emission (maximum at 340.5 nm, 3.64 eV, at 4.2 K) and a much stronger and broader emission band in the green part of the visible spectrum (maximum at about 500 nm, 2.5 eV, at 4.2 K), which is ascribed to recombination of a shallowly trapped electron with a deeply trapped hole.[12] As the size of the nanocrystal increases both bands shift to lower energies, reaching the bulk ZnO values (viz. 3.25 eV for the UV emission and ~2.5 eV for the visible emission) for particles with radii larger than 3 nm.[12] The size and temperature dependences of the photoluminescence of ZnO nanocrystals have been investigated in detail by Van Dijken *et al.*[12] and will not be addressed here. Oxygen vacancies have been assumed to be the most likely candidates for the recombination centers involved in the visible luminescence of ZnO,[12] but zinc vacancies have also been suggested. In the thermoluminescence only a broad emission band is observed which roughly coincides with the PL band. In Fig. 2(a) the open circles connected by the broken line indicate the intensity of the thermoluminescence in ZnO nanocrystals with a radius of 1.3 nm as a function of the temperature and it is seen that the maximum intensity occurs at 50–60 K where the reduction of the EPR signals is largest. After annealing at temperatures higher than 150 K the EPR lines of the shallow Li donor and the Na-related acceptor and the thermoluminescence are no longer observed. Note that after the UV excitation has been terminated the broad emission band is observable even at 5 K, but with its maximum shifted by approximately 0.1 eV to lower energy. Since this emission cannot be thermally induced at 5 K it is attributed to tunneling recombination between the electron and hole centers. The small shift in energy is explained by the fact that this recombination is not caused by excitation of the electron to the conduction band. This shift allows us to estimate the energy level of the shallow donor in ZnO nanocrystals with radii of 1.3 nm to be ~0.1 eV. This value is much larger than in bulk ZnO crystals where it was found that the interstitial hydrogen donor has an ionization energy of 35 meV.[3]

The comparison of the EPR/ENDOR experiments and the optical experiments show that the visible emission seems to be at least partly due to a charge-transfer transition of an electron from the shallow Li-related donor to the deep Na-related trap. The shape of the EPR signal II in Fig. 1 with a hyperfine (HF) interaction that is nearly isotropic suggests a HF interaction with a nucleus with spin $I=3/2$ with an almost 100% abundance. This observation favors a Na-related

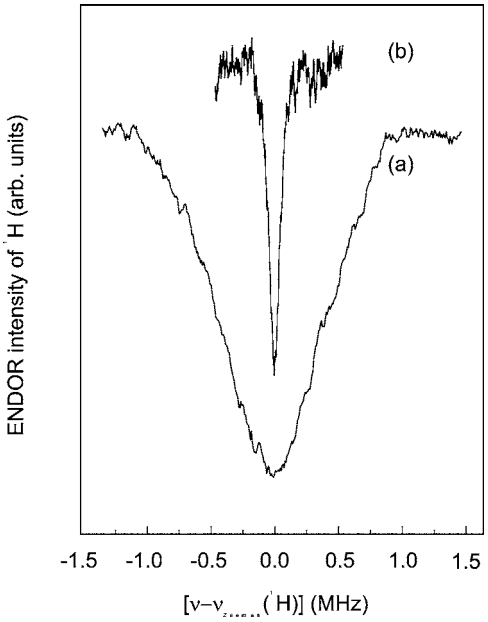

FIG. 3. The ENDOR transition of the ^{1}H nuclear spin observed at 94.9 GHz in the EPR signal II of the deep, Na-related acceptor (a) and in the EPR signal I of the shallow Li donor (b).

center and indeed the ENDOR study of this signal, as reported in our previous paper,[6] reveals two transitions at 4.2 MHz and 72.0 MHz. When neglecting the quadrupole interaction these two ENDOR frequencies are given by $\nu_{\mathrm{ENDOR}}=h^{-1}|g_n\beta_n B_0 \pm A/2|$, where $g_n\beta_n B_0/h$ is the Zeeman frequency for sodium. We thus find for the hyperfine constant $A=67.8$ MHz which corresponds to the HF splitting of 2.4 mT observed in the EPR line shape. This splitting of 2.4 mT is about 7% of the HF constant for free Na^0.[13]

The conclusion that this deep Na-related center is located close to or at the $ZnO/Zn(OH)_2$ interface is drawn from the observation that in the EPR signal II not only the ENDOR signals of the ^{23}Na ($I=3/2$) nucleus can be observed, but also the ENDOR signal of ^{1}H ($I=1/2$) nuclear spins [see curve (a) in Fig. 3]. The linewidth of 1.0 MHz is about 8 times larger than the linewidth of the ^{1}H ENDOR signals observed in the ESE-detected EPR signal of the shallow Li donor[6] [see curve (b) in Fig. 3]. This shows that the density of the electronic wave function of the Na-related acceptor is relatively large in the $Zn(OH)_2$ capping layer.

In Fig. 4 the effect is presented of saturating the ^{1}H nuclear-spin transition on the Na-related EPR signal. It is seen that the whole line shape undergoes a reduction in intensity demonstrating that the hyperfine interaction with the ^{1}H nucleus is related to the deep Na acceptor and not to an EPR signal of another center that might coincide with the signal of the Na-related acceptor.

In our previous paper[6] the deep Na-related center in ZnO was described as an oxygen vacancy adjacent to a substitutional Na impurity (V_O-Na_{Zn}). Formally such a construction could be a deep donor (an oxygen vacancy containing two electrons is neutral with respect to the normal O^{2-} site and is a double donor) and as a deep acceptor (Na_{Zn} is a deep acceptor).

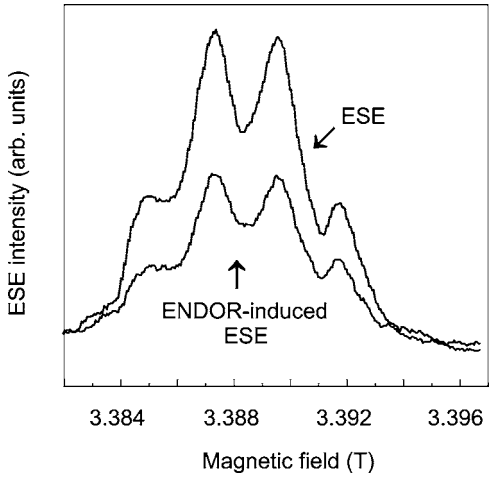

FIG. 4. A detailed recording of the ESE-detected EPR signal II of the deep Na-related acceptor (top line) at 94.9 GHz and a recording in the presence of a radio-frequency field that saturates the centre of the ENDOR line (ENDOR-induced ESE) of the ^{1}H nuclear spins (bottom line). During the sweep through the EPR line the frequency of the radio-frequency field is continuously adjusted to remain at the top of the ^{1}H ENDOR line. The reduction of the intensity of the complete EPR line by the applied radio-frequency field demonstrates that the ^{1}H ENDOR signal is connected to the Na-related EPR signal and not to another EPR signal that happens to coincide with signal II.

Before the UV illumination this center is not paramagnetic. Upon above-band-gap illumination an electron from the oxygen vacancy is transferred to the interstitial, shallow Li donor making both centers paramagnetic. Since we observe a relatively strong HF interaction of this localized Na-related center with a proton of the OH^- ligands of Zn in the capping layer we expect this vacancy-impurity complex to be located at or near to the $ZnO/Zn(OH)_2$ interface. The hole is then most probably located on Na because about 7% of the spin density is found on this atom.

The arguments leading to the assignment of signal III to the exchange-coupled pair of the shallow Li-donor and the deep Na-acceptor are the following. First its g value g_P is the average of the g values g_D of the shallow Li donor and the g value g_A of the deep Na acceptor: $g_P=\frac{1}{2}(g_D+g_A)$. This is the g value that one predicts for an exchange-coupled donor-acceptor pair when the exchange coupling $J \gg (g_D - g_A)\beta_e B_0$. In Fig. 1(b) the EPR spectrum recorded at 275 GHz is presented. The pair signal is again exactly halfway between the signals I and II, which are now separated by an interval that is larger by a factor 275/94.9=2.90. Second, the pair signal is only visible in ZnO nanoparticles with a radius smaller than 1.5 nm. Apparently, for these particles the exchange interaction that depends exponentially on the distance is large enough to create pairs visible in the EPR spectrum.

As mentioned above the EPR signals of the isolated shallow Li-interstitial donor and the Na-related deep acceptor decrease simultaneously and irreversibly when the temperature is increased. Simultaneously the EPR signal of the exchange-coupled pair starts to decrease irreversibly but al-

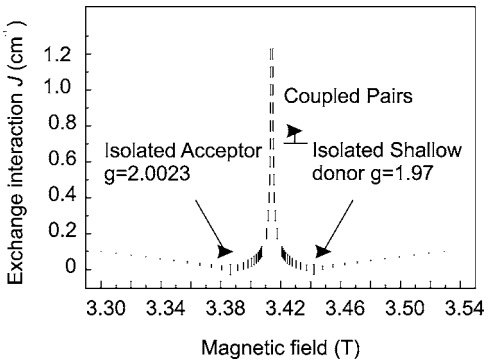

FIG. 5. The predicted positions for the EPR transitions at 94.9 GHz of two exchange-coupled particles with spins $S=1/2$ as a function of the absolute value of J. The g factors for the acceptor $g_A=2.0023$ and for the shallow donor $g_D=1.97$. The bar length corresponds to the EPR line intensity.

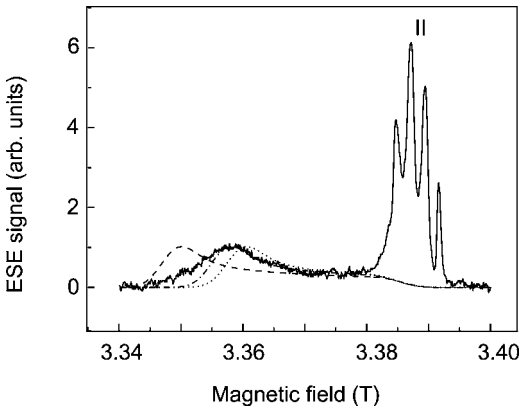

FIG. 6. The EPR spectrum taken at 94.9 GHz and at 1.5 K of deep acceptors in the core of ZnO nanocrystals with radii of 1.5 nm. The simulations for the Li_{Zn} deep acceptors (dashed line) and for the V_{Zn} deep acceptors (dotted line) have been produced using the parameters from Ref. 14. The dashed-dot line is the result of a fitting using $g_{\|}=2.0033$ and $g_{\perp}=2.0205$.

ready at lower temperatures. The signal completely disappears after annealing at 20 K. This could explain the low intensity of the pair signal observed at 275 GHz [Fig. 1(b)] because here the lowest temperature at which the EPR signal can be observed is 8 K compared to 1.5 K at 94.9 GHz. The difference in the intensity ratio of the EPR signal of I and II at 275 and 94.9 GHz (Fig. 1) is due to the difference in the nature of the EPR line broadening. The linewidth of the shallow donor is caused by g factor anisotropy which results in an increase of the linewidth at 275 GHz compared to 94.9 GHz and in a decrease of the signal intensity. The line width of the Na-related hole center is dominated by HF interaction which does not depend on the microwave frequency. As a result one observes the same intensity at 275 and 94.9 GHz.

Figure 5 shows the predicted magnetic-field positions of the EPR transitions at 94.9 GHz of two exchange-coupled spins $S=1/2$ of an acceptor with $g_A=2.0023$ and a donor with $g_D=1.97$ as a function of the absolute value of J. Such a coupled pair gives rise to a singlet and a triplet state with four possible EPR transitions. The bar length in Fig. 5 corresponds to the intensity of the EPR lines. The thick bars indicate the EPR lines of isolated acceptors and isolated shallow donors (i.e., $J=0$). The double thick bars in the center of the figure represent the two transitions of a strongly coupled pair. These transitions cannot be resolved in the EPR spectra due to the 5 mT linewidth of the shallow donors. They appear in the EPR spectrum when $J>0.7$ cm^{-1} and their position does not change appreciably when J is further increased. When J is varied between 5×10^{-3} and 0.7 cm^{-1}, the positions of the EPR lines change rapidly. As the value of J is decreased further, the EPR spectrum remains virtually unchanged and consists of two lines corresponding to the isolated donors and acceptors. Thus, EPR signals can be observed only in the case of strong ($J>0.7$ cm^{-1} at 94.9 GHz) and weak exchange coupling. For intermediate values of J, the positions of the EPR lines depend on J and, when averaged over all possible values of J, a broad spectrum results with a complicated shape and low intensity that is difficult to detect. We further conclude that the sign of J is negative because at 1.2 K the triplet state is observed.

The most probable position of the shallow interstitial Li donor with its large Bohr radius is near the center of a ZnO nanocrystal, while the deep Na-related acceptor is localized near the surface of the nanocrystal. Using the expression $J=J_0\exp(-2r/a_D)$ with $J_0=5.37$ cm^{-1} (see the Introduction) and using the radius of the nanoparticle $r=1.3$ nm we can estimate the exchange interaction J to be about 1 cm^{-1}. This is in a good agreement with the value derived from the simulated EPR line positions presented in Fig. 5.

We note that the Na-related surface acceptor is perhaps not the only deep acceptor that can capture the electron of the shallow Li donor because, as seen in Fig. 2, the intensity of the EPR signal of the deep Na acceptor decays somewhat faster than that of the shallow Li donor. As we have shown already in our previous paper[6] the EPR signal of an additional deep acceptor is observable with g factors that are typical for deep acceptors in ZnO bulk material. This signal is shown in Fig. 6 where also the signal of the deep Na-related surface acceptor is visible. We note that three types of deep acceptors in ZnO have similar structures and g values. These centers are respectively the substitutional Li or Na impurity (Li_{Zn} or Na_{Zn}), or the Zn vacancy (V_{Zn}).[14,15] ZnO has a wurtzite structure, with the Zn ions surrounded by distorted tetrahedrons of oxygen ions. The hole is located on one of the O^{2-} ligands and one thus has an O^{-} ligand with the unpaired spin located on one of the four p bonds. There are three nonaxial bonds that do not possess perfect axial symmetry and the g tensor of a hole on one of these three oxygen atoms is described by three different principal values g_Z, g_X, and g_Y. The oxygen in the c axis direction is inequivalent to the other three oxygen atoms, and the g tensor for a hole on this oxygen atom can be described by $g_{\|}$ and $g_{\perp}$. For the Li_{Zn} or Na_{Zn} impurities, the preferred site is the axial oxygen atom due to the energy difference between the axial and nonaxial state. For V_{Zn} acceptor only the nonaxial state was observed in bulk ZnO.[15]

We have compared the line shape of the EPR signal in Fig. 6 with a simulated curve using the known anisotropy of the g tensor of the deep Li_{Zn} and V_{Zn} acceptors[14,15] and as-

suming that the ZnO nanoparticles are randomly oriented. In Fig. 6 we present the simulations for the EPR line shapes of the deep Li_{Zn} acceptors with axial symmetry (dashed line) and for the Zn vacancy (V_{Zn}) deep acceptor (dotted line). The parameters used for Li_{Zn} are $g_{\|}=2.0028$, $g_{\perp}=2.0253$ and for V_{Zn} $g_Z=2.0033$, $g_X=2.0192$, $g_Y=2.0188$.[14,15] The dashed-dotted line results from a simulation using $g_{\|}=2.0033$, $g_{\perp}=2.0205$. In all simulations a linewidth was assumed of 5 mT. From a comparison of the simulated and the experimental curve we conclude that the EPR line in Fig. 6 originates either from the deep V_{Zn} or the deep Li_{Zn} acceptor or of a combination of these two centers. The simulated EPR spectrum of the Na_{Zn} acceptor deviates considerably from the experimental spectrum. The shape and position of the signal, presented in Fig. 6 is slightly sample dependent and we conclude that the main contribution to the signal is coming from the deep Zn vacancy acceptor which might be introduced during the growth of the nanocrystals. Thus this would represent the first direct observation of a vacancy in semiconductor nanocrystals induced during nanocrystal growth.

From the intensity of the EPR signals we conclude that upon illumination only one out of 10^3–10^4 particles carries a paramagnetic Li donor and a paramagnetic Na-related acceptor. The question then arises how it is possible to observe pairs in one nanocrystal. We propose that almost every ZnO nanocrystal contains an interstitial Li atom and a Na atom at the surface but that the Li atoms positioned not exactly at the center of the nanocrystal recombine so quickly with the Na-related surface acceptor that their EPR signals are not visible. This model explains why the EPR signals of the shallow Li donor and of the Na-related surface acceptor have about equal intensity because these centers only become paramagnetic upon illumination when an electron is transferred from the Na-related deep acceptor to the shallow Li donor.

A high concentration of Na-related acceptors is not unreasonable because it is a surface defect. These deep surface acceptors are probably introduced during the preparation of the nanocrystals by incorporation of Na impurities from the chemicals, solvents, and glassware. Surface adsorption of cations is very likely due to the large surface to volume ratio of nanocrystals and would be particularly favored during the precipitation, since the ZnO nanocrystals are negatively charged[16] what would provide a driving force for the nanocrystals to scavenge cations from solution upon addition of a low dielectric solvent such as heptane. Rinsing with heptane and acetone would probably succeed in removing small cations such as Li^+ from the surface but not large cations such as Na^+. This implies that even small Na concentrations would be effectively incorporated in the nanoparticles, making it difficult to prepare Na^+-free $ZnO/Zn(OH)_2$ nanocrystals. Indeed, even in ZnO nanocrystals synthesized in plasticware using compounds and solvents with the lowest commercially available concentration of Na impurities, the EPR signal of the deep Na acceptor is still present in comparable strength. Assuming that the incorporation of Na^+ is nearly quantitative ~35% of the 1.3 nm radius ZnO nanocrystals would contain a Na^+ ion, even at the lowest Na concentration achievable in our experiments.

An interesting observation is that EPR signals of the isolated shallow Li donor and of the isolated Na-related deep acceptor are present in addition to the signal of the exchange-coupled pair. We present three possible explanations. First, there is a spread in the radii of the nanoparticles of 10% and since the exchange interaction depends exponentially on the distance between the donor and the acceptor it is conceivable that in part of the particles the exchange interaction is too weak to form a pair. Second, there may be a distribution in the position of the Li donor in the particle. This may also lead to a spread in the exchange interaction. Third, it should be realized that the exchange interaction in the hexagonal ZnO structure most probably is anisotropic. This would imply that the size of the exchange interaction depends on the relative position of the Na-related acceptor with respect to the crystal axis. As a result in a part of the nanocrystals the exchange interaction may become so small that only the signals of the individual Li donors and Na-related acceptors are visible.

Finally we suggest that deep surface acceptors similar to the one observed in ZnO might be present in CdS and CdSe nanocrystals which are known to exhibit blinking behavior when a single nanocrystal is optically excited.[17] It is currently thought that such deep acceptors at the surface or in the capping layer of CdS and CdSe nanoparticles are essential to explain the lengthening of the "on" periods in the blinking. It would be interesting to study CdS and CdSe nanoparticles with EPR and ENDOR techniques to corroborate this suggestion.

CONCLUSION

The combination of EPR and optical experiments allows us to demonstrate that donor-acceptor pairs are formed in the confined structure of ZnO nanoparticles between the shallow, interstitial Li donor and a deep Na-related acceptor. From ENDOR experiments it is concluded that these deep acceptors are located at the $ZnO/Zn(OH)_2$ interface. Moreover we supply arguments that make us believe that deep Zn-vacancy related deep acceptors are incorporated in the ZnO nanocrystals during growth.

ACKNOWLEDGMENTS

This work forms part of the research program of the Netherlands Foundation for Fundamental Research of Matter (F.O.M.) and the Technology Foundation STW, with financial support from the Nederlandse Organisatie voor Wetenschappelijk Onderzoek (N.W.O.). Financial support from the SENTINEL Network in the framework of the 5th EC Science Program is acknowledged. P.G.B. acknowledges support by RFBR under Grants No. 04-02-17632 and No. 05-02-17817, and Programs of RAS Spintronics, Quantum Macrophysics and Quantum Nanoscience.

[1] F. C. Rong, W. A. Barry, J. F. Donegan, and G. D. Watkins, Phys. Rev. B **54**, 7779 (1996); W. A. Barry and G. D. Watkins, *ibid.* **54**, 7789 (1996), and references therein.
[2] N. M. Atherton, in *Principles of Electron Spin Resonance* (Horwood, London, 1993).
[3] Detlev M. Hofmann, Albrecht Hofstaetter, Frank Leiter, Huijan Zhou, Frank Henecker, Bruno K. Meyer, Serguei B. Orlinskii, Jan Schmidt, and Pavel G. Baranov, Phys. Rev. Lett. **88**, 045504 (2002).
[4] R. T. Cox and J. J. Davies, Phys. Rev. B **34**, 8591 (1986).
[5] O. G. Poluektov, M. C. J. M. Donckers, P. G. Baranov, and J. Schmidt, Phys. Rev. B **47**, 10226 (1993).
[6] S. B. Orlinskii, J. Schmidt, P. G. Baranov, D. M. Hofmann, C. de Mello Donegá, and A. Meijerink, Phys. Rev. Lett. **92**, 047603 (2004).
[7] S. B. Orlinskii, J. Schmidt, E. J. J. Groenen, P. G. Baranov, C. de Mello Donegá, and A. Meijerink, Phys. Rev. Lett. **94**, 097602 (2005).
[8] J. A. J. M. Disselhorst, H. J. van der Meer, O. G. Poluektov, and J. Schmidt, J. Magn. Reson., Ser. A **115**, 183 (1995).
[9] H. Blok, J. A. J. M. Disselhorst, S. B. Orlinskii, and J. Schmidt, J. Magn. Reson. **166**, 92 (2004).
[10] H. Blok, J. A. J. M. Disselhorst, H. van der Meer, S. B. Orlinskii, and J. Schmidt, J. Magn. Reson. **173**, 49 (2005).
[11] W. B. Mims, in *Electron Paramagnetic Resonance*, edited by S. Geschwind (Plenum, New York, 1972).
[12] Addy van Dijken, Eric A. Meulenkamp, Daniël Vanmaekelbergh, and Andries Meijerink, J. Phys. Chem. B **104**, 1715 (2000).
[13] J. R. Morton and K. F. Preston, J. Magn. Reson. **30**, 577 (1978).
[14] O. F. Schirmer and D. Zwingel, Solid State Commun. **8**, 1559 (1970).
[15] A. L. Taylor, G. Filipovich, and G. K. Lindeberg, Solid State Commun. **8**, 1359 (1970).
[16] E. A. Meulenkamp, J. Phys. Chem. B **102**, 5566 (1998).
[17] M. Nirmal, B. O. Dabbousi, M. G. Bawendi, J. J. Macklin, J. K. Trautman, T. D. Harris, and L. E. Brus, Nature (London) **383**, 802 (1996).